Diffusion studies with synchrotron radiation

2001 J. Phys.: Condens. Matter 13 7763

(http://iopscience.iop.org/0953-8984/13/34/319)

INSTITUTE OF PHYSICS PUBLISHING JOURNAL OF PHYSICS: CONDENSED MATTER

J. Phys.: Condens. Matter **13** (2001) 7763–7774 PII: S0953-8984(01)26755-1

Diffusion studies with synchrotron radiation

Gero Vogl and Markus Hartmann

Hahn-Meitner Institut, Glienickerstrasse 100, D-12053 Berlin, Germany
and
Institut für Materialphysik der Universität Wien, Strudlhofgasse 4, A-1090 Wien, Austria

Received 6 July 2001
Published 9 August 2001
Online at stacks.iop.org/JPhysCM/13/7763

Abstract

In this article we want to present the basic ideas of (microscopic) diffusion studies. It is the aim of such investigations to reveal the basic jump processes, i.e., to find the elementary jump vectors and jump frequencies. In this paper we first present a historic introduction, explaining the fundamental ideas of diffusion by presenting the work of Fick and Einstein. Then we introduce the basics of scattering theory (Van Hove), that are later on used to obtain an expression for the scattering function of a system of diffusing particles (Chudley and Elliott, Singwi and Sjölander). Until the mid-1990s this scattering function was measured as a function of wavevector transfer and energy. But the rise of synchrotron sources with their pulsed radiation and the parallel development of detectors and monochromators finally provided the possibility of studying the intermediate scattering function directly, i.e., measuring the scattered intensity as a function of wavevector transfer and *time*. We present this relatively new method of nuclear resonant scattering of synchrotron radiation in the forward direction together with two examples: the diffusion of iron in the intermetallic alloys Fe_3Si and FeAl.

1. Introduction—some historical facts

Diffusion, i.e., the effort of nature to equalize concentration gradients, is a widely studied field. Approximately 200 years ago Jean Baptiste Fourier (1768–1830) and Adolf Fick (1829–1901) found the fundamental equation for particle diffusion. The driving force for particle wandering, i.e., diffusion, is assumed to be a concentration gradient. The simplest way of combining these facts is the following linear *ansatz*[1]

$$\boldsymbol{j} = -D\,\boldsymbol{\nabla} c(\boldsymbol{x}, t) \qquad \text{(Fick's first law)}. \tag{1}$$

$\boldsymbol{j}$ denotes the particle flux (i.e., number of particles per area and time), c the concentration of particles (i.e., number of particles per volume) which is a function of space and time, and D is the so-called diffusion coefficient. It is measured in $m^2\ s^{-1}$. Fick's first law applies

[1] Here and elsewhere in the article, vectors are denoted by bold type.

to all non-ballistic viscous flow of particles in a gradient field, such as thermal conductance, electrical conductance (Ohm's law), and viscous flow of fluids.

If particle conservation is demanded, one obtains another equation—a so-called 'continuity equation'—that further restricts Fick's first law. Since there are no sources and drains for particles, the flux of particles through the boundary S of a volume V must result in an equivalent change in the number of particles in that volume, i.e.,

$$\frac{\partial}{\partial t}\int_V c(\boldsymbol{x},t)\,\mathrm{d}V = -\int_S \boldsymbol{j}\cdot\mathrm{d}\boldsymbol{S} \overset{\text{Stokes}}{=} -\int_V \boldsymbol{\nabla}\cdot\boldsymbol{j}\,\mathrm{d}V. \tag{2}$$

One obtains

$$\frac{\partial}{\partial t}c(\boldsymbol{x},t) + \boldsymbol{\nabla}\cdot\boldsymbol{j} = 0 \qquad \text{(continuity equation)}. \tag{3}$$

Substituting this last equation into Fick's first law (1), one obtains Fick's second law, the well known 'diffusion equation':

$$\frac{\partial}{\partial t}c(\boldsymbol{x},t) = D\,\Delta c(\boldsymbol{x},t) \qquad \text{(Fick's second law)}. \tag{4}$$

This equation is solved by

$$c(\boldsymbol{x},t) = (4\pi Dt)^{-3/2}\exp\left(-\frac{\boldsymbol{x}^2}{4Dt}\right) \tag{5}$$

with the initial condition[2] $c(\boldsymbol{x}, t=0) = \delta(\boldsymbol{x})$. In figure 1, $c(\boldsymbol{x},t)$ is plotted for several times t. One can recognize that the concentration profile smears out with time—in the limit of very long timescales being completely flat with zero concentration gradient.

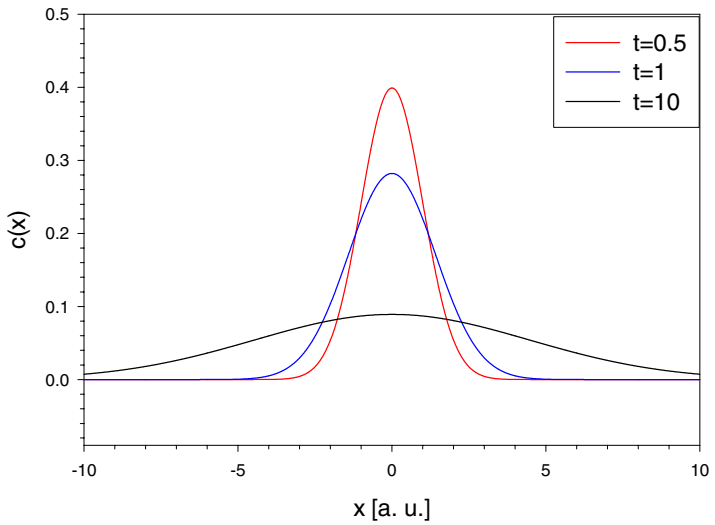

Figure 1. The concentration profile at different times, demonstrating the broadening of the curve.

Fourier's and Fick's ideas were completely rooted in the concept of 'continuous matter'. The idea of atoms forming our world in physics had its breakthrough at the end of the 19th

[2] The solution for arbitrary initial condition $c(\boldsymbol{x}, t=0) = f(\boldsymbol{x})$ is given by

$$c(\boldsymbol{x},t) = f(\boldsymbol{x}) * \left[(4\pi Dt)^{-3/2}\exp\left(-\frac{\boldsymbol{x}^2}{4Dt}\right)\right]$$

where '$*$' denotes the convolution of two functions.

century essentially because of the Viennese physicist Ludwig Boltzmann (1844–1906), who developed a statistical theory of heat to explain the fundamental laws of thermodynamics. In the year 1905 Albert Einstein (1879–1955) used Boltzmann's ideas to develop a molecular kinetic concept of Brownian motion that could be observed in suspended particles in a liquid [4]. In the atomistic view, this motion should be the result of many stochastic collisions between the molecules of the liquid and the suspended particle. In the first part of his work, Einstein calculated the diffusion coefficient of the suspended particles just in terms of particle radius r, viscosity of the liquid η, and temperature T:

$$D = RT(6\pi N\eta r)^{-1} \tag{6}$$

where R stands for the universal gas constant and N for Avogadro's number.

In the second part of the work Einstein connects the motion of the particles in the liquid with diffusion. It is informative to follow Einstein's argumentation (in one dimension). It is assumed that the motion of one particle at the time t is independent of the motion of all other particles and of the motion of the same particle at former times (Markov process). Now define τ to be a time interval which is small compared to measuring times, but big enough to ensure that the motions of the particle in two consecutive time intervals are independent of each other. Then define n to be the number of suspended particles and Δ to be the increase (positive or negative) in a particle's x-coordinate during τ. It is clear that Δ will have a different value for each particle. Now there will be a special probability $\varphi(\Delta)$ of a particle undergoing an increase in its x-coordinate of Δ. Then the following three conditions hold for the function $\varphi(\Delta)$:

(1) $\int_{-\infty}^{\infty} \varphi(\Delta)\,\mathrm{d}\Delta = 1$;
(2) $\varphi(\Delta) = \varphi(-\Delta)$;
(3) $\varphi(\Delta) \approx 0$ (for Δ big enough).

For the concentration of particles at position x and time $t + \tau$, the definition of φ yields

$$c(x, t+\tau) = \int_{-\infty}^{\infty} c(x+\Delta, t)\varphi(\Delta)\,\mathrm{d}\Delta.$$

Taylor expansion of both sides of this equation yields

$$c + \frac{\partial c}{\partial t}\tau = c\underbrace{\int_{-\infty}^{\infty} \varphi(\Delta)\,\mathrm{d}\Delta}_{=1\text{ (equation (1))}} + \frac{\partial c}{\partial x}\underbrace{\int_{-\infty}^{\infty} \Delta\varphi(\Delta)\,\mathrm{d}\Delta}_{=0\text{ (equation (2))}} + \frac{\partial^2 c}{\partial x^2}\int_{-\infty}^{\infty} \frac{\Delta^2}{2}\varphi(\Delta)\,\mathrm{d}\Delta. \tag{7}$$

By setting

$$\tau^{-1}\int_{-\infty}^{\infty} \frac{\Delta^2}{2}\varphi(\Delta)\,\mathrm{d}\Delta \equiv D \tag{8}$$

one obtains

$$\frac{\partial c}{\partial t} = D\frac{\partial^2 c}{\partial x^2} \tag{9}$$

which is nothing else than Fick's second law.

At the end of these considerations, probably the most famous equation for tracer diffusion is presented, that for the mean square displacement (MSD), i.e., the mean distance that a particle travels away from the origin as a function of time. It is given by the second moment of the concentration distribution $c(\boldsymbol{x}, t)$:

$$\langle \boldsymbol{x}^2 \rangle = \int \boldsymbol{x}^2 c(\boldsymbol{x}, t)\,\mathrm{d}^3x = 6Dt. \tag{10}$$

Therefore measuring the MSD as a function of time provides information about the diffusion coefficient D.

2. Scattering measurements

So far we have only considered 'free' diffusion (i.e., the atoms could move freely and continuously through space), a concept that is valid on scales of length and time that are large compared to atomic scales. Today we know that the atoms that build up matter are very often arranged in a lattice. This leads to the new concept of 'jump diffusion', i.e., the atoms have to perform jumps from one lattice point to another instead of moving continuously through space. This new view of the diffusion concept leads to new challenges in science, e.g., the determination of jump vectors and jump frequencies that could be used to predict the macroscopic diffusion coefficient D. Tracer diffusion proved to be no perfect tool for investigating the atomic details of diffusion. Tracer diffusion is very insensitive to the single-atomic motion because it averages over many jumps. In this section we wish to describe scattering experiments, which proved to be the ultimate instrument for gaining information on the microscopic details of the diffusion process, as are tracer experiments on the macroscopic scale.

The principles of a scattering experiment are easily explained: an incoming beam of particles (waves) is fired onto a sample, where the particles (waves) interact with the sample atoms ('they are scattered'). The outgoing intensity of particles (waves) is measured as a function of angle (wavevector transfer $\boldsymbol{Q}$) and ω (energy transfer) (see figure 2).

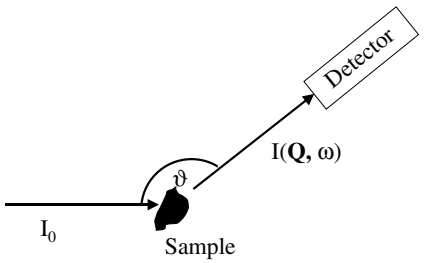

Figure 2. The principle of a scattering experiment: the incoming beam hits the sample and the scattered intensity is measured as a function of angle and energy.

On the other hand it is a formidable theoretical task to connect the measured scattering function $S(\boldsymbol{Q}, \omega)$ with the atomic details of the sample. In 1954 Léon Van Hove published a work [30] that has radically influenced modern physics, for it has become the foundation of all modern scattering experiments. Therein he showed that there is a close connection between the correlation function of a system and the scattering function of the same system, more exactly

$$G(\boldsymbol{r}, t) = (2\pi)^{-3} \int S(\boldsymbol{Q}, \omega) \exp(-\mathrm{i}(\boldsymbol{Q} \cdot \boldsymbol{r} - \omega t))\, \mathrm{d}^3\boldsymbol{Q}\, \mathrm{d}\omega \tag{11}$$

where $G(\boldsymbol{r}, t)$ stands for the 'Van Hove correlation function' and $S(\boldsymbol{Q}, \omega)$ denotes the scattering function, i.e., the probability for a particle to undergo a wavevector transfer of $\boldsymbol{Q}$ and an energy transfer of $\hbar\omega$ in the scattering process. The correlation function $G(\boldsymbol{r}, t)$ measures the probability of finding any particle at position $\boldsymbol{r}$ at time t when there was a particle at the origin at time zero. Equation (11) simply states that the scattering function is the spatial and temporal Fourier transform of the correlation function. The intermediate scattering function $I(\boldsymbol{Q}, t)$ is defined by a *single* Fourier transform of $G(\boldsymbol{r}, t)$ in space:

$$I(\boldsymbol{Q}, t) = \int \exp(-\mathrm{i}\boldsymbol{Q} \cdot \boldsymbol{r}) G(\boldsymbol{r}, t)\, \mathrm{d}\boldsymbol{r}. \tag{12}$$

One can extract the self-correlation function $G_s(\boldsymbol{r}, t)$, which measures the probability of finding the same atom at position $\boldsymbol{r}$ at time t when it was at the origin at time zero:

$$G(\boldsymbol{r}, t) = G_s(\boldsymbol{r}, t) + G_d(\boldsymbol{r}, t). \tag{13}$$

$G_d(\boldsymbol{r}, t)$ stands for the 'distinct' part of the correlation function, i.e., the probability of finding another particle at $(\boldsymbol{r}, t)$, when there was some particle at (0, 0). For more details, see, e.g., [12].

It is this self-correlation function that plays a crucial role in the theory of diffusion, because it describes the wandering of atoms. Equation (5) is nothing but the self-correlation function for large timescales (remember Einstein's argumentation, leading to Fick's second law by evaluating the probability of a particle increasing its x-coordinate). Thus for large timescales, when the details of the atomic jump processes are smeared out, $G_s(\boldsymbol{r}, t)$ has to fulfil the diffusion equation (4).

But we are interested in the microscopic details of the diffusion process, i.e., in the jump vectors and jump frequencies. The next section explains how the correlation formalism can be applied to diffusion on an atomic scale and how the desired information can be extracted from the measured quantities.

3. Jump diffusion on a lattice

It is the aim of this section to generalize the concept of continuous, i.e., macroscopic, diffusion to the microscopic, i.e., atomic, scale, where the atoms are arranged in a lattice. This is done in terms of a correlation function so that the Van Hove formalism can be applied easily. The method goes back to the work of Chudley and Elliott [3] and Singwi and Sjölander [28].

Hence let us consider an ensemble made up of atoms that jump between the sites of a Bravais lattice. We assume that the residence time τ—the time for which an atom stays on a special lattice site—is very large compared to the jump time; so the latter is neglected. Additionally we assume that only nearest-neighbour jumps are possible; the extension is straightforward.

Therefore we write $\boldsymbol{l}_k$ for the jump vector to nearest-neighbour sites. In terms of a rate equation (see, e.g., [31]) the probability of finding an atom at lattice point $\boldsymbol{r}$ at time t—together with the boundary condition $G_s(\boldsymbol{r}, 0) = \delta(\boldsymbol{r})$, nothing else than the self-correlation function[3]—reads

$$\frac{\partial}{\partial t} G_s(\boldsymbol{r}, t) = \frac{1}{n\tau} \sum_{k=1}^{n} [G_s(\boldsymbol{r} + \boldsymbol{l}_k, t) - G_s(\boldsymbol{r}, t)] \tag{14}$$

where each lattice site has n nearest neighbours. $1/\tau$ is called the jump rate.

Equation (14) is solved by transforming into $\boldsymbol{Q}$-space (see equation (12)):

$$\frac{\partial}{\partial t} I(\boldsymbol{Q}, t) = -\frac{1}{n\tau} \sum_{k=1}^{n} \left[1 - \exp(\mathrm{i}\boldsymbol{Q} \cdot \boldsymbol{l}_k)\right] I(\boldsymbol{Q}, t) \tag{15}$$

with

$$I(\boldsymbol{Q}, t) = \int_{-\infty}^{\infty} G_s(\boldsymbol{r}, t) \exp(-\mathrm{i}\boldsymbol{Q} \cdot \boldsymbol{r})\, \mathrm{d}\boldsymbol{r}. \tag{16}$$

Equation (15) exploits the fact that

$$\hat{G}_s(\boldsymbol{r} + \boldsymbol{a}) = \exp(\mathrm{i}\boldsymbol{k} \cdot \boldsymbol{a}) \hat{G}_s(\boldsymbol{r}) \tag{17}$$

where $\hat{G}$ denotes the Fourier transform of G. With the abbreviation

$$\Delta\omega(\boldsymbol{Q}) = \frac{1}{n\tau} \sum_{k=1}^{n} \left[1 - \exp(\mathrm{i}\boldsymbol{Q} \cdot \boldsymbol{l}_k)\right] \tag{18}$$

equation (15) is solved by

$$I(\boldsymbol{Q}, t) = \exp(-\Delta\omega(\boldsymbol{Q})\, t) \tag{19}$$

[3] Appearing directly in QMS and QNS and less directly in nuclear resonant scattering of synchrotron radiation.

which is nothing else than an exponential decay in time. Another Fourier transform—now in t instead of $\boldsymbol{r}$—yields

$$S(\boldsymbol{Q}, t) = \frac{1}{\pi} \frac{\Delta\omega(\boldsymbol{Q})}{\omega^2 + (\Delta\omega(\boldsymbol{Q}))^2} \tag{20}$$

a Lorentzian with a FWHM of $2\,\Delta\omega(\boldsymbol{Q})$.

Of course this formalism can be applied to the more general case of non-Bravais lattices (for example, see [21], [15] or [20]; further information can be found in [5, 19]). In these cases the notation becomes a bit clumsy, because one has to be aware of several sublattices and therefore of sites with different symmetry, which leads to a lot of indexing on the jump vectors. The crucial result of such an analysis is that the functions S and I become superpositions of several Lorentzians and exponentials respectively (one for each sublattice).

Now let us investigate equations (19) and (20) more closely. These two equations describe exponentials and Lorentzians with $\boldsymbol{Q}$-dependent decay rates and linewidths respectively (more exactly: the shapes of the curves depend on the scalar product of $\boldsymbol{Q}$ and the jump vector $\boldsymbol{l}$ and on the jump frequency τ; see equation (18)). For example on a Bravais lattice, where for each jump vector $\boldsymbol{l}$, $-\boldsymbol{l}$ is also a jump vector (inversion symmetry), equation (18) reduces to

$$\Delta\omega(\boldsymbol{Q}) = \frac{4}{n\tau} \sum_{\boldsymbol{l}_k > 0} \sin^2\left(\frac{\boldsymbol{Q} \cdot \boldsymbol{l}_k}{2}\right). \tag{21}$$

Therefore measuring the decay of the intermediate scattering function (19) and the linewidth of the scattering function (20) in various directions provides information on the elementary diffusion process.

Before we show examples of real measurements, we want to give an intuitive picture of how one can understand the diffusional accelerated decay and line broadening: if the timescales of the scattering process and of the diffusion process (jump frequencies) match, with the result that during the scattering process the scattering particle undergoes several diffusion jumps, the emitted (scattered) wave is cut into several wave trains. These wave trains now interfere with each other, prevalently leading to a loss of intensity, i.e., destructive interference, and therefore giving rise to the phenomenon of line broadening in energy space and accelerated decay in time space. Only in very special directions, when the path-length differences of the emitted wave trains (i.e. the scalar products of $\boldsymbol{Q}$ and $\boldsymbol{l}$) are integral multiples of the wavelength of the incident particles, can constructive interference can be maintained, which leads to sharp lines and slow decays.

4. Measurements

Now that we have developed the theoretical concepts of diffusion, it is time to present experimental results. There are three experimental methods that proved to be adequate to study diffusion in the way described:

(1) Quasielastic neutron scattering (QNS).
(2) Quasielastic Mössbauer spectroscopy (QMS).
(3) Nuclear resonant scattering of synchrotron radiation (NRS).
(4) Neutron spin-echo spectroscopy (NSE).

In this work we wish to focus on the relatively new method of NRS (see, e.g., [26] or [17]); information on QNS and QMS and recent results can be found in, e.g., [8, 9, 27, 32]. Further information on NSE can be found in [18] or [10]. Resonant methods, such as QMS or NRS, provide the extraordinarily good energy resolution that makes these methods so valuable.

Conventional Mössbauer spectroscopy (working with a radioactive source and absorber) did not provide the opportunity to work in the time domain (i.e., measuring the intermediate scattering function), because it did not provide a time structure[4]. It was the rise of synchrotrons with their pulsed radiation and the parallel development of detectors and monochromators that finally provided the possibility to study the intermediate scattering function directly.

Performing a resonant experiment with a strongly coherent beam is a bit more tricky than performing the scattering measurements described in section 2. Because of the strong coherent properties of the incoming beam, all resonant atoms are coherently excited ('nuclear exciton') and therefore emit the radiation coherently in the forward direction. The nuclei act as sources for the radiation and therefore the coherence may be destroyed if the atom performs a diffusive jump during the emission process ('the atom takes the phase with it'). One may regard a resonant scattering process as a process where the incoming pulse is very short compared to the scattering process itself, contrary to the case for a classical scattering experiment (e.g., QNS), where the opposite is true, the incoming beam being quasicontinuous and the scattering process being extremely short. For more details, see, e.g., [7, 13, 14, 29]. Figure 3 illustrates the situation.

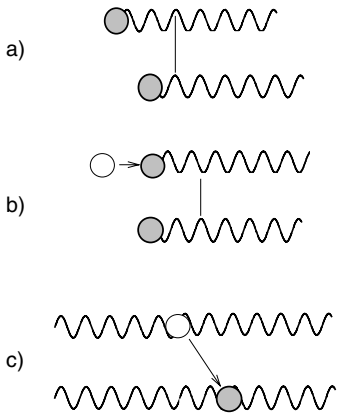

Figure 3. In (a) one sees two nuclei that are coherently excited and therefore emit γ-radiation coherently in the forward direction, i.e., without any path-length difference. In (b) one of these atoms performs a jump, which leads to a path-length difference of the two wave trains and therefore to a loss of coherence. One should bear in mind that the atoms in (a) and (b) act as sources and consequently take their phase with them, whereas in (c) the situation that occurs in, e.g., QNS is shown: the incoming beam is quasicontinuous and the scattering process so short that a jumping atom does not destroy the coherence in the forward direction. That is why QNS measurements cannot be performed in the forward direction.

In our case we used the 14.4 keV level of ^{57}Fe with a natural lifetime of 141 ns and measured the number of delayed quanta as a function of time. All of the experiments were carried out at the Nuclear Resonance Beamline of the ESRF (for details on the beamline, see [22]). The synchrotron was run in 16-bunch mode, providing a radiation pulse with a duration of about 100 ps every 176 ns. The change of the slope of the decay with increasing temperature was measured in various directions. For the set-up, see figure 4. In this paper we present the results for Fe_3Si (reference [26]) and FeAl (reference [24]).

[4] In 1991 a Russian group succeeded to chop the incident nuclear radiation from a Mössbauer source and so to produce artificially a time structure of the Mössbauer radiation [36]

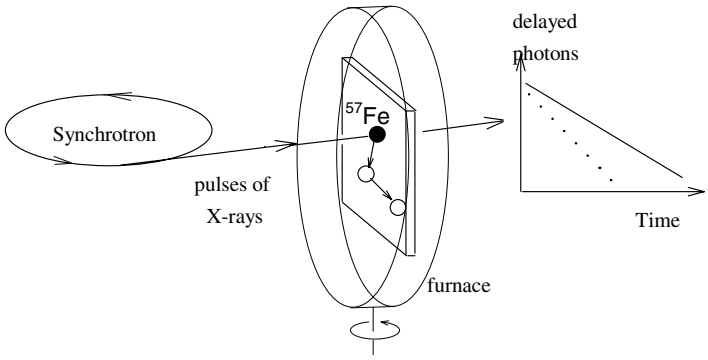

Figure 4. The set-up of a NRS experiment. Note that the orientation of the crystal axis with respect to the synchrotron beam can be chosen freely. Full line: number of delayed photons at low temperatures. Dotted line: accelerated decay in the presence of diffusion at elevated temperatures.

4.1. Fe_3Si

The measurements were done on a Fe_3Si single crystal which was cut with its surface parallel to the (113) direction. Fe_3Si crystallizes in the so-called $D0_3$ structure, which is shown in figure 5. This structure consists of three sublattices occupied by iron (α_1-, α_2-, and γ-sites) and one sublattice occupied by silicon (β-sites). The iron atoms are assumed to perform jumps on the iron sublattice only, giving rise to up to three exponentials, which sum up to the scattering function. But there are also some degenerate directions where only two ([113]) or even just one ([111]) exponential is observable. The measurements were performed in these directions to minimize the uncertainties. The results can also be seen in figure 5. The measurements, which constituted a feasibility test for the new method, confirmed the older results from QMS that had identified the elementary jump mechanism of iron atoms as being jumps between the α- and β-sublattices avoiding the silicon sublattice.

4.2. FeAl

The intermetallic stoichiometric alloy FeAl was chosen because of its great interest for diffusion studies. In contrast to Fe_3Si, FeAl crystallizes in the $B2$ structure (see figure 7, later) and therefore all nearest neighbours of iron are aluminium atoms. An extensively discussed problem concerns the question of whether the iron atoms jump directly from one iron site to another (regardless of the long paths) or whether they briefly occupy the energetically unfavourable Al antisites (see, e.g., [35]). Earlier experiments with QMS suggested the latter [6, 23, 33], with a preference for [110] jumps over [100] jumps. Because up to now first-principles calculations were not able to reproduce such a jump mechanism, it appeared necessary to check the results from QMS with the new method of NRS.

A stoichiometric single crystal of FeAl was prepared and oriented with its $(1\bar{1}0)$ plane horizontal, i.e., in the plane of the synchrotron beam. Figure 6 shows the measurements in the (110) direction for four different temperatures. To gain the required information on jump vectors and jump frequencies it was necessary to measure the curve in many different directions. Because of the limited beam time it was not possible to follow the intensity decay over a long time interval, so another method was adopted: time integration of the intensity. The idea is that a faster decay will lead to a smaller integrated intensity than a slow one without diffusion. ODIN (orientation dependence of the integrated intensity of NRS) was chosen as

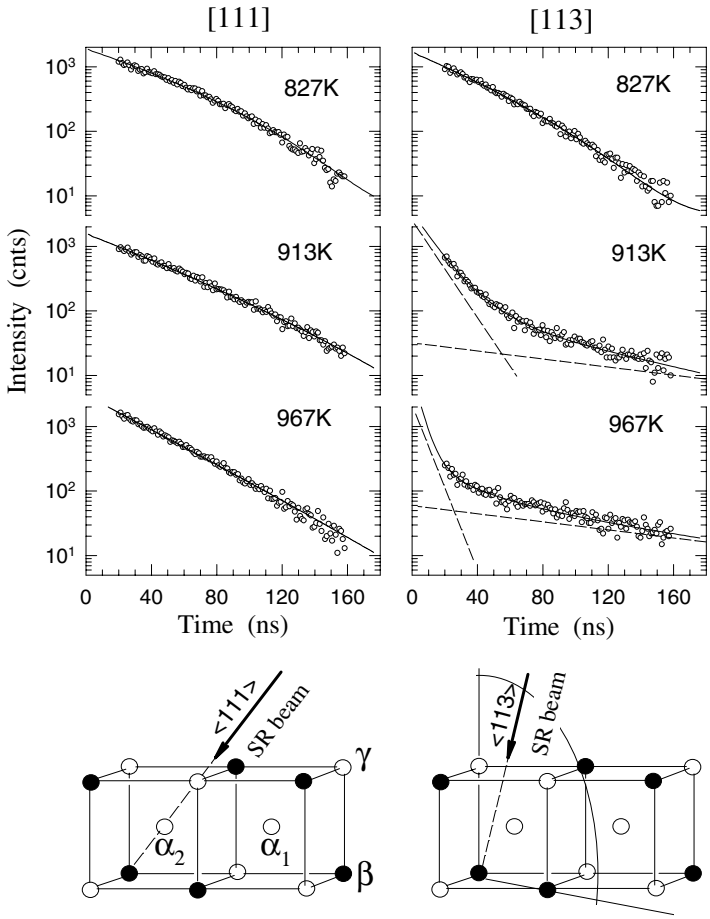

Figure 5. Top: results for the Fe_3Si measurements. The intermediate scattering function was measured in two directions, [111] and [113]. In the first direction, there is only one exponential decay, which is hardly accelerated by diffusion. In the [113] direction the scattering function consists of two exponentials; one of them shows an accelerated decay that becomes stronger with increasing temperature. Bottom: 2/8 of the elementary cell of Fe_3Si. The white circles denote iron sites, the full circles the silicon sublattice. We also show in which direction the beam hit the sample. (This figure was taken from [34].)

the name for this method.

Figure 7 shows the results of our measurements. The best fit is achieved by assuming a combination of [110] and [100] jumps in the ratio (1.9 ± 0.1):1. The measurements show that the effective jumps of the diffusion stay on the iron sublattice. Even though it cannot be directly decided whether the diffusing iron atoms take the roundabout way over the Al antisites with a much shorter residence time on the Al sites or not, all considerations regarding the underlying mechanism that lead to the measured combination of [110] and [100] jumps lead to the conclusion that a nearest-neighbour jump to an antistructure site on the Al sublattice must be the elementary jump (as indicated in figure 7). If the antisite was not used it would not be possible to explain the favouring of [110] jumps. On the other hand, there are first-principles calculations that find this jump to an antistructure site too costly in energy [16]; this is why these authors introduce double jumps or six-jump cycles to explain the experimental results.

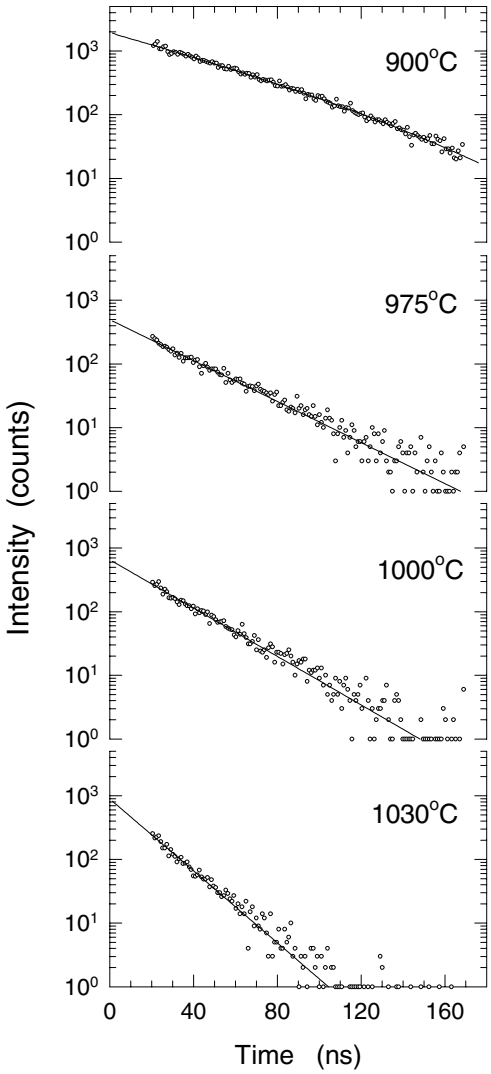

Figure 6. Measurements of FeAl in the (110) direction. The acceleration of the decay with increasing temperature is clearly visible. (This figure was taken from [24].)

4.3. Outlook

For further experiments with synchrotron radiation, it seems desirable to extend the investigations to alloys not containing iron. Two methods appear to be very promising: time domain interferometry (TDI) and speckle spectroscopy. In TDI measurements one uses stainless steel foils in front of and behind the sample which are in constant relative motion. The coherent excitation of these two foils produces an artificial beat pattern which is destroyed by diffusive processes in the sample [1, 11, 25].

Speckle spectroscopy is a technique known from laser spectroscopy that makes use of the outstanding coherent properties of laser light. Because of the large wavelength of laser light ($\approx 10^4$ Å) it was mostly used to study systems large on the atomic scale (e.g., particles suspended

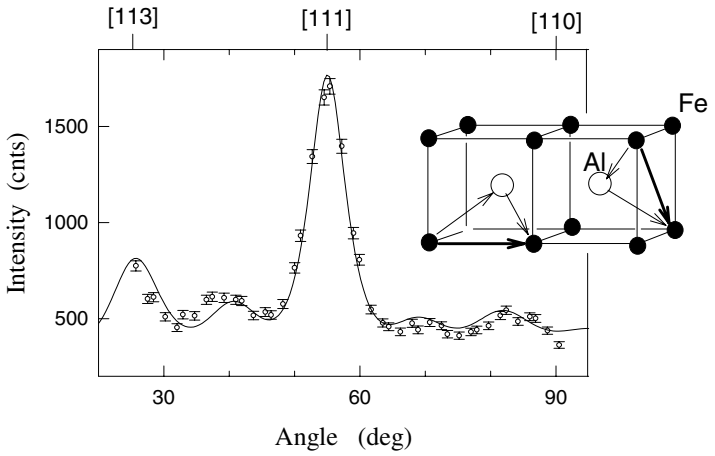

Figure 7. ODIN for FeAl. The fit presented is the best one, achieved by a combination of effective [110] and [100] jumps with a ratio of (1.9 ± 0.1):1. (This figure was taken from [34].)

in a liquid). With the upgrade of modern synchrotrons it seems possible to extend this method to synchrotron radiation and therefore to a much shorter wavelength ($\approx$1 Å), so slow atomic motions should in principle be observable. Speckle spectroscopy is completely non-resonant, so measurements can be carried out on almost all systems. Speckle measurements have already been successfully made with synchrotron radiation; e.g., see [2] where critical fluctuations near the phase transformation were measured.

Acknowledgments

The authors wish to express their thanks for many enlightening discussions to Bogdan Sepiol, Martin Kaisermayr, Marcel Sladecek and Lorenz Stadler.

References

[1] Baron A Q R, Franz H, Meyer A, Rüffer R, Chumakov A I, Burkel E and Petry W 1997 Quasielastic scattering of synchrotron radiation by time domain interferometry *Phys. Rev. Lett.* **79** 2823

[2] Brauer S, Stephenson G B, Sutton M, Brüning R, Dufresne E, Mochrie S G J, Grübel G, Als-Nielsen J and Abernathy D L 1995 X-ray intensity fluctuation spectroscopy observations of critical dynamics in Fe_3Al *Phys. Rev. Lett.* **74** 2010

[3] Chudley C T and Elliott R J 1961 Neutron scattering from a liquid on a jump diffusion model *Proc. Phys. Soc.* **77** 353

[4] Einstein A 1905 Über die von der molekularkinetischen Theorie der Wärme geforderte Bewegung von in ruhenden Flüssigkeiten suspendierten Teilchen *Ann. Phys., Lpz.* IV **17** 549

[5] Feldwisch R 1996 Elementarsprung der Eisendiffusion in intermetallischen Eisen-Aluminium-Legierungen—Quasielastische Mössbauerspektroskopie an geordneten und ungeordneten Phasen *PhD Thesis* Universität Wien

[6] Feldwisch R, Sepiol B and Vogl G 1995 Elementary diffusion jump of iron atoms in intermetallic phases studied by Mössbauer spectroscopy—II. From order to disorder *Acta Metall. Mater.* **43** 2033

[7] Hannon J P and Trammel G T 1999 Coherent γ-ray optics *Hyperfine Interact.* **123+124** 127

[8] Kaisermayr M, Combet J, Ipser H, Schicketanz H, Sepiol B and Vogl G 2000 Nickel diffusion in $B2$-NiGa studied with quasielastic neutron scattering *Phys. Rev.* B **61** 12 038

[9] Kaisermayr M, Combet J, Ipser H, Schicketanz H, Sepiol B and Vogl G 2001 Determination of the elementary jump of Co in CoGa by quasielastic neutron scattering *Phys. Rev.* B **63** 054303

[10] Kaisermayr M, Pappas C, Triolo A, Sepiol B and Vogl G 2001 Neutron spin-echo probes diffusion on lattices, submitted
[11] Kaisermayr M, Sepiol B, Thiess H, Vogl G, Alp E E and Sturhahn W 2001 Time-domain interferometry of synchrotron radiation for diffusion in intermetallic alloys *Eur. Phys. J.* B **20** 335
[12] Kehr K 1996 Streufunktionen $S(\boldsymbol{Q}, \omega)$ und Korrelationsfunktionen *Streumethoden zur Untersuchung kondensierter Materie (27 IFF-Ferienkurs Forschungszentrum Jülich)*
[13] Kohn V G and Smirnov G V 1998 Theory of nuclear resonant scattering of synchrotron radiation in the presence of diffusive motion of nuclei. II *Phys. Rev.* B **57** 5788
[14] Kohn V G and Smirnov G V 1999 Synchrotron radiation time spectra affected by diffusion: theory *Hyperfine Interact.* **123+124** 327
[15] Kutner R and Sosnowska I 1977 *J. Phys. Chem. Solids* **38** 741
[16] Mayer J and Fähnle M 1997 Investigation of self-diffusion in B_2-FeAl and $D0_3$-Fe_3Al by the *ab-initio* electron theory *Defect Diffus. Forum* **143–147** 285
[17] Meyer A, Franz H, Wuttke J, Petry W, Wiele N, Rüffer R and Hübsch C 1997 Nuclear resonant scattering of synchrotron radiation for the study of dynamics around the glass transition *Z. Phys.* B **103** 479
[18] Mezei F 1980 *Neutron Spin Echo* ed F Mezei (Berlin: Springer)
[19] Randl O G, Sepiol B, Vogl G and Feldwisch R 1994 Quasielastic Mössbauer spectroscopy and quasielastic neutron scattering from non-Bravais lattices with differently occupied sublattices *Phys. Rev.* B **49** 8768
[20] Richter D, Hempelmann R and Schönfeld C 1991 *J. Less-Common Met.* **172–174** 595
[21] Rowe J M, Sköld K, Flotow H E and Rush J J 1971 Quasielastic neutron scattering by hydrogen in the α and β phases of vanadium hydride *J. Phys. Chem. Solids* **32** 41
[22] Rüffer R and Chumakov A I 1996 Nuclear Resonance Beamline at ESRF *Hyperfine Interact.* **97+98** 589
[23] Sepiol B 1993 Atomic jumps in ordered intermetallic compounds *Phys. Scr.* T **49** 378
[24] Sepiol B, Czihak C, Meyer A, Vogl G, Metge J and Rüffer R 1998 Synchrotron radiation study of diffusion in FeAl *Hyperfine Interact.* **113** 449
[25] Sepiol B, Kaisermayr M, Thiess H, Vogl G, Alp E E and Sturhahn W 2000 Quasielastic scattering of synchrotron radiation from non-resonant atoms *Hyperfine Interact.* **126** 329
[26] Sepiol B, Meyer A, Vogl G, Rüffer R, Chumakov A I and Baron A Q R 1996 Time domain study of ^{57}Fe diffusion using nuclear forward scattering of synchrotron radiation *Phys. Rev. Lett.* **76** 3220
[27] Sepiol B and Vogl G 1993 Atomistic determination of diffusion mechanism on an ordered lattice *Phys. Rev. Lett.* **71** 731
[28] Singwi K S and Sjölander A 1960 Resonance absorption of nuclear gamma rays and the dynamics of atomic motions *Phys. Rev* **120** 1093
[29] Smirnov G V and Kohn V G 1995 Theory of nuclear resonant scattering of synchrotron radiation in the presence of diffusive motion of nuclei *Phys. Rev.* B **52** 3356
[30] Van Hove L 1954 Correlations in space and time and Born approximation scattering in systems of interacting particles *Phys. Rev.* **95** 249
[31] van Kampen N G 1992 *Stochastic Processes in Physics and Chemistry* (Amsterdam: Elsevier Science)
[32] Vogl G and Feldwisch R 1998 The elementary diffusion step in metals studied by methods from nuclear solid state physics *Diffusion in Condensed Matter* ed J Kärger, P Heitjans and R Haberlandt (Braunschweig: Vieweg) p 40
[33] Vogl G and Sepiol B 1994 Elementary diffusion jump of iron atoms in intermetallic phases studied by Mössbauer spectroscopy—I. Fe–Al close to equiatomic stoichiometry *Acta Metall. Mater.* **42** 3175
[34] Vogl G and Sepiol B 1999 Diffusion in crystalline materials *Hyperfine Interact.* **123+124** 595
[35] Vogl G, Sepiol B, Czihak C, Rüffer R, Weinkamer R, Fratzl P, Fähnle M and Meyer B 1998 Microscopic diffusion mechanism of iron in FeAl revisited by new methods *Diffusion Mechanism in Crystalline Materials* ed Y Mishin, G Vogl, N Cowern, R Catlow and D Farkas (Pittsburgh, PA: Materials Research Society) p 197
[36] Shvydko Y V, Smirnov G V, Popov S L and Hertrich T 1991 *Pis. Zh. Eksp. Teor. Fiz.* **53** 69 (Engl. Transl. 1991 *JETP Lett.* **53** 69)